JOC The Journal of Organic Chemistry

Article

pubs.acs.org/joc

Photochromism of *o*-Nitrophenyl-Substituted Oxazabicycles

Wen-Chung Lin and Ding-Yah Yang*

Department of Chemistry, Tunghai University, No. 1727, Sec. 4, Taiwan Boulevard, Xitun District, Taichung 40704, Taiwan, Republic of China

Supporting Information

ABSTRACT: The *o*-nitrophenyl-substituted oxazabicycle **1** was prepared via a one-pot tandem multicomponent reaction. Upon exposure to UV light in CH_2Cl_2, it turned purple and reverted back to its original color while being heated. The in situ trapping of the photogenerated product with trimethylsilyl cyanide yielded the adduct **4**, which confirmed the formation of the ring-opened zwitterionic species **2**. The EPR spectroscopic data, PBN spin-trapping experiments, and spectroelectrochemical studies of the model compound **7** provided evidence to support that the photochromism of **1** involved the zwitterionic biradical intermediate **5**, generated by photoinduced intramolecular electron transfer from the amine moiety to the nearby *o*-nitrophenyl group. Further, two photogenerated side products responsible for the photofatigue of **1** were isolated and characterized, and a possible mechanism for their formation was proposed.

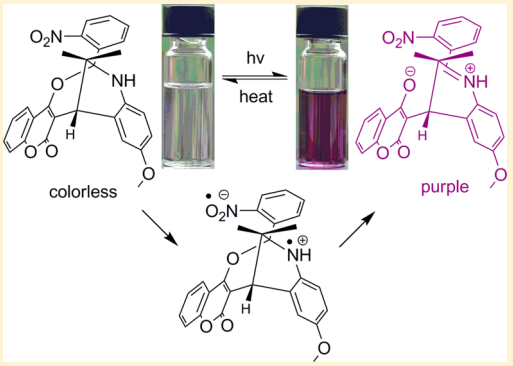

INTRODUCTION

The field of organic photochromism has continued to attract considerable attention, since compounds with photochromic properties may have wide applications in the areas of photonic materials[1] and optical memory devices.[2] Typical photochromic compounds include diarylethenes,[3] spiropyrans,[4] azobenzenes[5]/overcrowded ethenes,[6] and others.[7] Their reversible reactions between two bistable states involve electrocyclic reactions, intramolecular cyclizations, and *cis*−*trans* photoisomerizations, respectively. While in the literature various compounds have been reported to exhibit photochromism, the development of photochromic colorants with novel molecular scaffolds as well as new photochromic mechanisms remains highly desired. We recently reported the oxazabicycle-based photochromic colorant **1**, which can be converted to the corresponding ring-opened product **2** upon UV irradiation (Scheme 1).[8] In this report, we demonstrate that the photochromism displayed by this *o*-nitrophenyl-substituted oxazabicycle **1** in methylene chloride rests on photoinduced intramolecular electron transfer from the electron donor amine to the electron acceptor *o*-nitrophenyl group. Thus, in contrast to the known photochromic systems, a reversibly formed zwitterionic biradical species is proposed as the intermediate. We describe herein photochemical, spin-trapping, and spectroelectrochemical studies, which have been used for the detection, characterization, and elucidation of the mechanism of this novel photochromism. Further, we have isolated and characterized two photogenerated side products responsible for the photofatigue of **1** and showed that all of the experimental observations can be accounted for by the formation of a photochemically created zwitterionic biradical intermediate.

Scheme 1. Photochromism of the Oxazabicycle 1

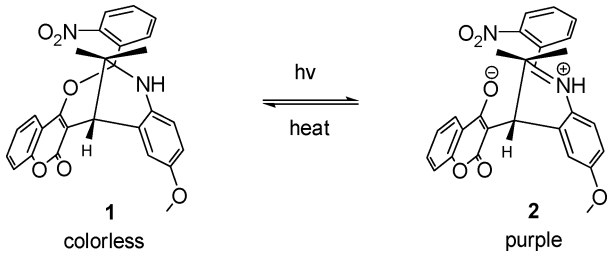

RESULTS AND DISCUSSION

Synthesis and Crystal Structures. Scheme 2 describes the one-pot tandem synthesis of the oxazabicycle **1** and its

Scheme 2. One-Pot Synthesis of the Oxazabicycle 1 and Its Methylated Product 3

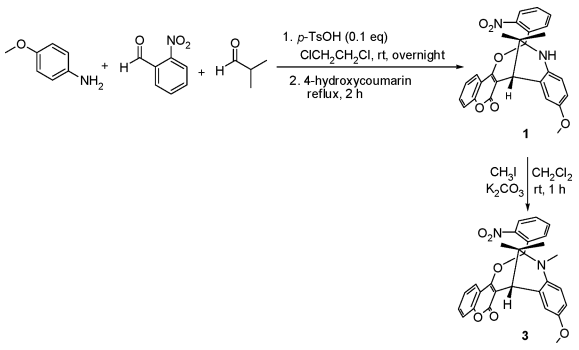

Received: August 20, 2013
Published: November 4, 2013

dx.doi.org/10.1021/jo401838n | J. Org. Chem. 2013, 78, 11798−11806

methylated product **3**. Compound **1** was readily prepared by mixing *p*-anisidine with *o*-nitrobenzaldehyde, isobutyraldehyde, and 0.1 equiv of *p*-TsOH in 1,2-dichloroethane at room temperature overnight, followed by treating with 4-hydroxycoumarin under reflux conditions.[9] Further reaction of **1** with iodomethane in methylene chloride at room temperature in the presence of potassium carbonate as a base afforded the corresponding N-methylated product **3**. Figure 1 shows the X-ray crystal structures of both **1** and **3**.[10] They share similar conformations with the *o*-nitro group of the bridgehead benzene ring oriented opposite to the amine moiety.

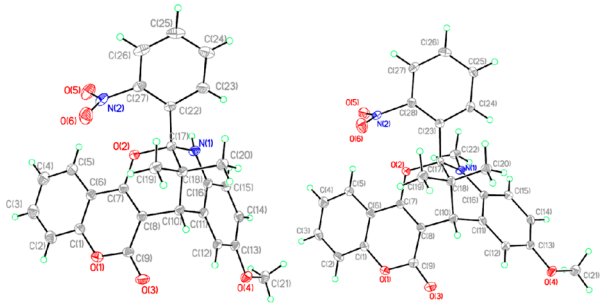

Figure 1. X-ray crystal structures of **1** and **3**.

Photochemical Properties. Upon ultraviolet irradiation (352 nm), the oxazabicycle **1** in CH_2Cl_2 turned from colorless to purple, as shown in Figure 2. With an increase of exposure

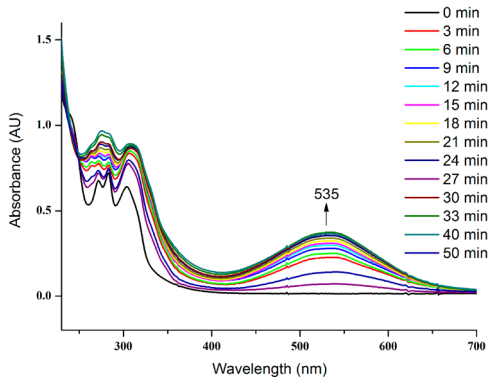

Figure 2. Absorption spectra of **1** (8.5×10^{-5} M in CH_2Cl_2) obtained with different exposure times (352 nm), 0−50 min, with increments of 3−10 min.

time, a new absorption band with a peak wavelength of around 535 nm gradually increased. When it sat in the dark or was heated, the photogenerated product in CH_2Cl_2 thermally decayed with the disappearance (i.e., turning colorless) of the 535 nm band. Isolation of the photogenerated product proved to be difficult, since it reverted easily back to the original form on the silica gel column. The zwitterionic species **2** has been previously assigned to be the major photogenerated product on the basis of the results of molecular simulation studies utilizing the density functional theory (DFT) method under full geometry optimization (B3LYP/6-31G*). According to Figure 2, no isosbestic point was observed during photolysis of **1**. This result implies the formation of byproducts with the irradiation of light (352 nm). Indeed, being solely dependent on the change of 535 nm absorbance from the zwitterionic species **2**, the production of **2** was found to decrease to ∼50% of its first photoconversion after the fourth cycle. These observations suggest that the UV light irradiation of the colorless species **1** may also give rise to the photochemical reaction of the colored species **2**. Presumably, the photogenerated product **2**, in a small percentage, may undergo either aromatization to give a quinoline derivative or light-induced deoxygenation of the *o*-nitrophenyl group to form an indazole derivative upon UV irradiation, which results in a less satisfactory reversible switching between the colorless species **1** and the colored species **2**.[8]

Trapping of the Zwitterionic Form and Characterization. To provide more evidence to support the formation of the zwitterionic species **2** upon irradiation of **1**, the photogenerated product was subjected to in situ trimethylsilyl cyanide (TMSCN) trapping experiments,[11] as shown in Scheme 3. Although attempts to acquire the X-ray crystal

Scheme 3. Trapping of the Photogenerated Product by TMSCN

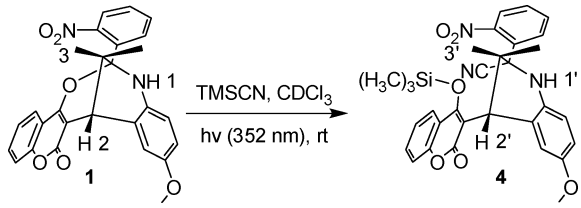

structure of the proposed adduct **4** were futile, the dynamic proton NMR studies did unambiguously reveal its formation. Figure 3 shows the time-dependent partial ^{1}H NMR spectra of **1** in the presence of excess TMSCN prior to and after UV irradiation. Before irradiation, a broad peak at chemical shift of 5.06 ppm was assigned to the amine hydrogen (H1 of **1**) absorption (see Scheme 3 for hydrogen atom labeling). The signal became much sharper and was slightly shifted upfield to 5.02 ppm (H1′ of **4**) after irradiation. Further, the bridgehead hydrogen (H2 of **1**) shifted downfield from 3.79 to 3.81 ppm to the ring-opened hydrogen H2′ of the adduct **4**. Finally, the most discernible signal variations were the absorptions of two *gem*-dimethyl groups. Upon irradiation, one shifted upfield from 1.07 to 1.00 ppm and the other downfield from 1.13 to 1.19 ppm, which might result from the drastic environmental change after ring opening and TMSCN trapping. The formation of adduct **4** was almost quantitative, and the reaction was complete within 35 min. This result coincides with the DFT calculations and supports the formation of the zwitterionic species **2** as the major photogenerated product. Interestingly, the TMSCN-trapped adduct **4** was found to gradually revert back to the ring-closed **1** via elimination of TMSCN on storage in the dark for 2 days (Figure 3, spectra f and g). This observation suggests that the oxazabicycle **1** is thermodynamically more stable than the adduct **4**, even though the former is surrounded by excess TMSCN.

As for the ^{13}C NMR spectra of **4** (see the Supporting Information), in addition to the observation of the cyano carbon absorption at 117.7 ppm, the bridgehead carbon that was attacked by the cyanide ion and the *gem*-dimethyl-substituted quaternary carbon were found to shift downfield from 106.0 ppm to either 110.4 or 108.5 ppm (indistinguishable) and from 34.6 to 41.0 ppm, respectively. Ultimately, the

dx.doi.org/10.1021/jo401838n | J. Org. Chem. 2013, 78, 11798−11806

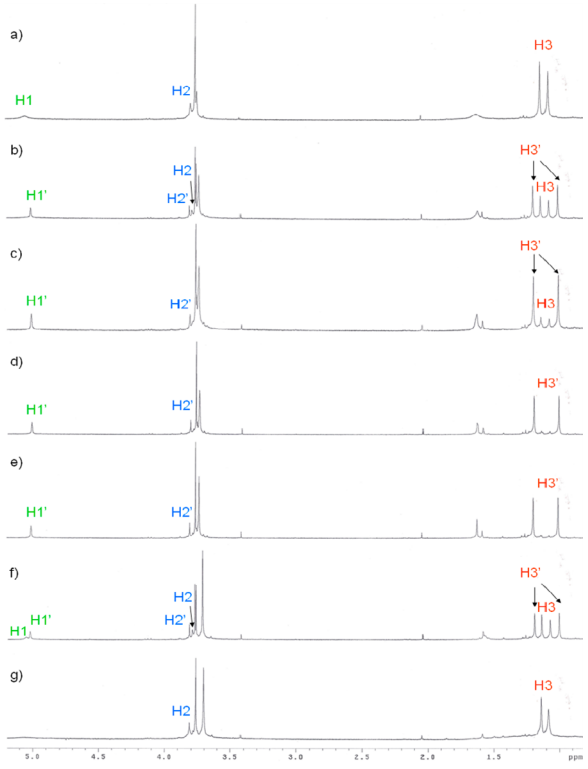

Figure 3. Partial ^{1}H NMR spectra (300 MHz, $CDCl_3$) of **1** (1.4×10^{-2} M) in the presence of 10 equiv of TMSCN after irradiation (352 nm) for (a) 0 min, (b) 10 min, (c) 15 min, (d) 25 min, and (e) 35 min and after storage in the dark for (f) 24 h and (g) 48 h. The peak at around 3.7 ppm corresponds to HCN absorption.

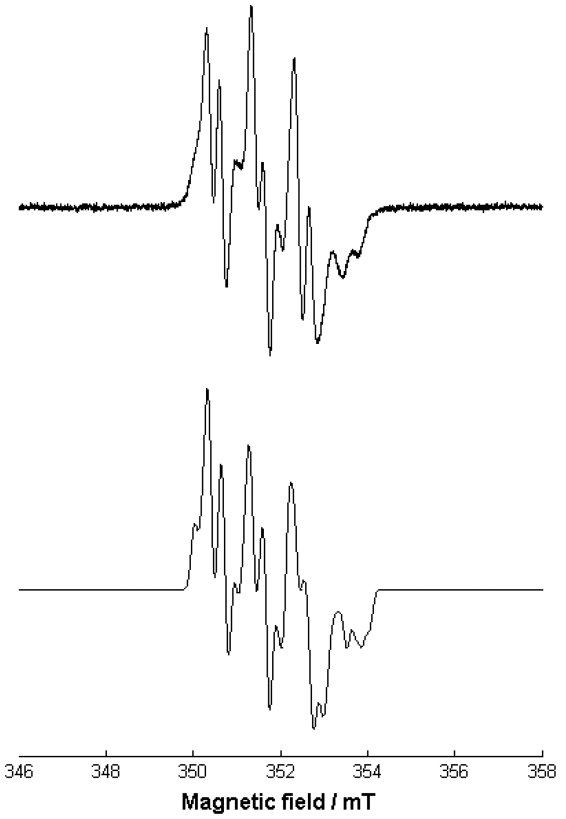

Figure 4. (top) EPR spectrum of **1** in degassed CH_2Cl_2 after irradiation with a 365 nm UV source at room temperature. (bottom) Simulated spectrum by EasySpin. Simulation parameters were performed with *hfc* anisotropy and *g*-factor anisotropy as follows: HFC tensor $\mathbf{A}_N$ = [0.82 0.86 1.00] mT, $\mathbf{A}_H$ = [0.29 0.29 0.28] mT, and **g** tensor = [2.0043 2.0027 2.0042]; the additional line width was 0.15 mT.

detection of the molecular ion at *m*/*z* 569.2 by ESI-MS also supported the formation of TMSCN adduct **4**.

EPR Measurements. Having confirmed that the photogenerated product indeed is the zwitterionic species **2**, we turned our attention toward the mechanism of this photochromism by subjecting the oxazabicycle **1** to EPR spectral measurements. Figure 4 (top) depicts the EPR spectrum of **1** recorded in degassed CH_2Cl_2 solution at room temperature under irradiation (365 nm). In the absence of UV light, no apparent EPR signals were observed. Upon irradiation, EPR signals were clearly detected. The intensity of the signals, centered around 351.5 mT (g = 2.0062), increased when the exposure time increased. This observation suggests that the photochemical reaction of **1** involves, at least in part, a radical species as the transient intermediate. In an effort to gain the information for the molecular structure of the radical intermediate, spectral simulation using the software package EasySpin[12] was carried out and the results are shown in Figure 4 (bottom). The simulated spectra exhibit an α-hydrogen hyperfine constant of 0.29 mT and an average nitrogen hyperfine coupling constant of 0.89 mT. The latter is close to the reported values for the ethoxyquin aminyl radical (0.80 mT),[13] the phenylaminyl radical (0.795 mT),[14] and the *N*-*tert*-butyl-*p*-methoxyphenylaminyl radical (0.94 mT).[15] The observed and simulated EPR data imply the formation of a radical species centered on the anisidine nitrogen atom during photoirradiation of **1**. It is worth mentioning that the compound with the nitro group of **1** substituted at the *para* position of the benzene ring and the methylated **3** were both nonphotochromic and EPR silent under the same irradiation conditions, indicating that the *o*-nitrophenyl group and the adjacent secondary amine of **1** play key roles in its light-sensitive properties.[16]

On the basis of the EPR experiments, a plausible mechanism for the photochromic switch between **1** and **2** is proposed as outlined in Scheme 4. It begins with single-electron transfer (SET) from the amine nitrogen of **1** to the *o*-nitrophenyl group to yield the zwitterionic biradical **5**. The subsequent ring opening of **5** via homolytic cleavage of the C−O bond gives the biradical iminium **6**. Final back electron transfer (BET) from the negatively charged nitro group to the oxygen radical atom on coumarin affords the zwitterionic species **2**. Presumably, both **5** and **6** may be responsible for the observed EPR signals.[17]

Electrochemistry and Spectroelectrochemical Studies. To gain more evidence to support the proposed radical mechanism for this photochromism, the electrochemical properties of **1** were explored. Figure 5 shows the cyclic voltammetry (CV) measurements of **1** at room temperature in CH_3CN at a scan rate of 100 mV s^{-1}, in which an irreversible redox process with oxidation potential of +0.97 V vs Ag/AgCl was observed. We speculate that the electrochemical studies of **1** may be complicated by the presence of the bridgehead C−O bond and the coumarin moiety in the oxazabicyclic skeleton. Thus, the two structurally simplified amino alcohols **7** and **8** (Figure 6) were subsequently prepared as model compounds to

dx.doi.org/10.1021/jo401838n | J. Org. Chem. 2013, 78, 11798−11806

Scheme 4. Proposed Photochromic Mechanism between 1 and 2

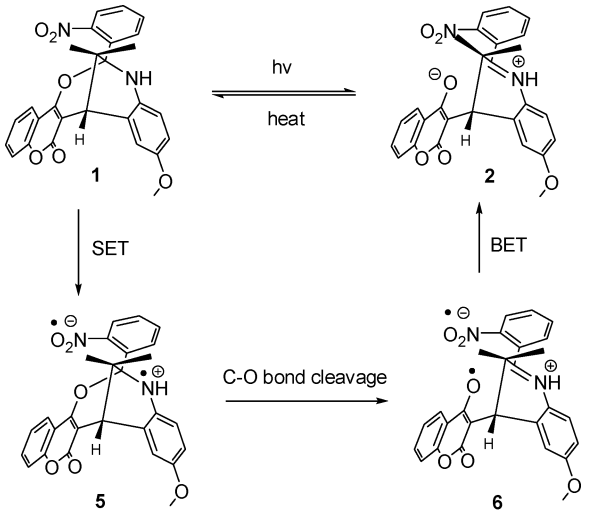

SET: single electron transfer; BET: back electron transfer

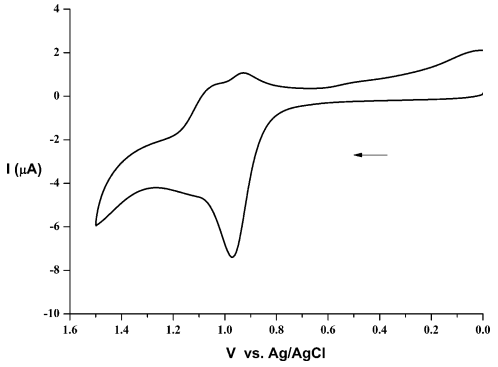

Figure 5. Electrochemical measurements for **1** performed at room temperature in CH_3CN containing $TBAPF_6$ (0.1 M) as supporting electrolyte. Potentials (V) are reported versus Ag/AgCl with reference to the ferrocence/ferrocenium (Fc/Fc^+) couple (CH_3CN, 25 °C, +0.57 V) at a scan rate of 100 mV/s.

investigate their photochemical and spectroelectrochemical properties.[8,10]

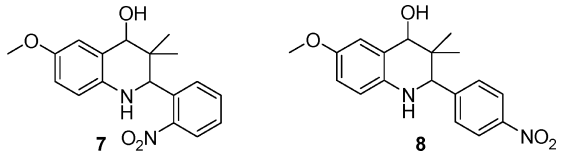

Figure 6. Structures of the model compounds **7** and **8**.

Figure 7 depicts the EPR spectrum of **7** (top) recorded in degassed CH_2Cl_2 at room temperature under UV irradiation (352 nm) and the simulated spectrum by EasySpin (bottom). Compound **7** was found to be EPR-active with splitting patterns similar to those of **1**. The simulated EPR spectrum of **7** exhibits an α-hydrogen and average nitrogen hyperfine constants of 0.36 and 0.90 mT, respectively. Conversely, compound **8** is EPR-silent under the same measuring conditions. The observation of highly similar EPR spectra of **1** and **7** suggests that the photogenerated radical species upon

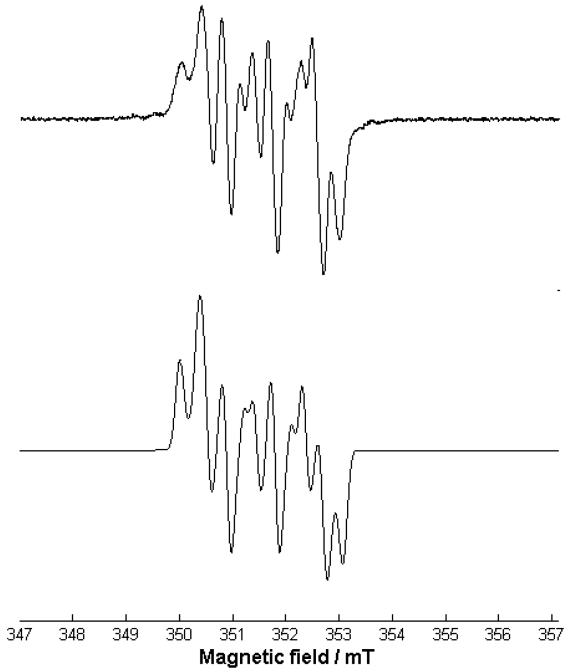

Figure 7. (top) EPR spectrum of **7** in degassed CH_2Cl_2 at room temperature, recorded immediately after irradiation with a 365 nm UV source. (bottom) Simulated spectrum by EasySpin. Simulation parameters were performed with *hfc* anisotropy and *g* factor anisotropy as follows: HFC tensor $\mathbf{A}_N$ = [0.89 0.92 0.89] mT, $\mathbf{A}_H$ = [0.36 0.36 0.35] mT, and **g** tensor = [2.0087 2.0055 2.0033]; the additional line width was 0.17 mT.

UV irradiation of both compounds share similar molecular structures. Presumably, the EPR signals of **7**, like those of compound **1**, resulted from the EPR-active zwitterionic biradical species generated by photoinduced intramolecular electron transfer from the electron donor amine to the electron acceptor *o*-nitrophenyl group. As for compound **8**, no EPR signals were observed, simply because the donor amine and the acceptor *p*-nitro group are not in close proximity for electron transfer to occur.

Figure 8 shows the CV measurements (top) and spectroelectrochemical spectra (bottom) of **7**. A one-electron reversible oxidation half-wave potential (+0.69 V vs Ag/AgCl) was observed at a scan rate of 100 mV s^{-1}, which corresponds to the removal of one electron from the anisidine nitrogen atom to form a cation radical. To further elucidate the formation of this cation radical species as the transient intermediate of the electrochemical oxidation of **7**, the in situ UV−vis spectroelectrochemistry was measured. When a potential (+0.95 V) was applied to **7**, a long-wavelength broad absorbance band at around 479 nm in the UV−vis spectrum, which resembles the absorption behavior of the aniline nitrogen radical,[18] was clearly detected, along with the appearance of an isosbestic point at 263 nm. The recovery rate was found to be up to 95% when the applied external potential was lowered to +0.45 V.

The gathered EPR, CV, and spectroelectrochemical data demonstrate that compound **7** is sensitive to light and is prone to undergo either photochemical or electrochemical oxidation by losing an electron from the anisidine nitrogen atom to yield a colored cation radical species.[19] In light of the great structural and conformational resemblance of the *o*-nitrophenyl amine moieties between **7** and **1**, along with the fact that both

dx.doi.org/10.1021/jo401838n | J. Org. Chem. 2013, 78, 11798−11806

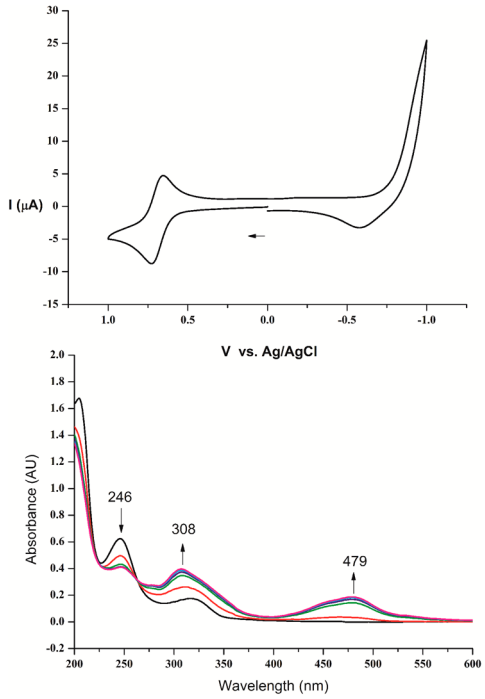

Figure 8. (top) Electrochemical measurements for **7** performed at room temperature in CH_3CN containing $TBAPF_6$ (0.1 M) as supporting electrolyte. Potentials (V) are reported versus Ag/AgCl with reference to the ferrocence/ferrocenium (Fc/Fc^+) couple (CH_3CN, 25 °C, +0.57 V) at a scan rate of 100 mV/s. (bottom) Spectral changes of **7** in CH_3CN containing $TBAPF_6$ (0.1 M) at an applied potential of +0.95 V. The spectra were recorded at 30 s intervals.

compounds share similar HOMO−LUMO electron populations (Figures S2 and S3 in the Supporting Information) and spin density distribution[20] (Figure S4 in the Supporting Information) patterns calculated by DFT, it is reasonable to assume that **7** and **1** may also exhibit similar photochemical properties: that is, to undergo photoinduced intramolecular electron transfer upon UV irradiation.

Spin Trapping of the Biradical Intermediate. To further confirm the existence of the radical intermediate shown in Scheme 4, the EPR spin-trapping technique was employed to detect the proposed biradical species. When the EPR measurements were performed for **1** in the presence of an excess of the spin-trapping agent *α*-phenyl-*N*-*tert*-butyl nitrone (PBN) at room temperature, no signals were observed prior to UV irradiation. In contrast, upon irradiation it showed clear EPR signals with two hyperfine couplings (Figure 9, A_N = 1.35 mT, A_H = 0.175 mT), which resulted from the splitting with nitrogen and benzylic hydrogen on the PBN moiety. These values are in good agreement with those reported in the literature for radical adducts.[21] Scheme 5 shows the proposed structure of the spin-trapped adducts **9** and **10**. Signals corresponding to the bisadducts of PBN were not observed under these conditions.

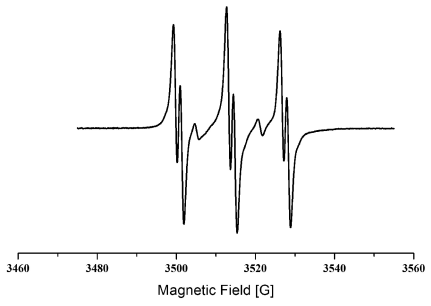

Figure 9. EPR spectra of spin-trapped adducts obtained upon UV irradiation (365 nm) of **1** and PBN in CH_2Cl_2 at room temperature.

Scheme 5. Proposed Structures of the Spin-Trapped Adducts 9 and 10

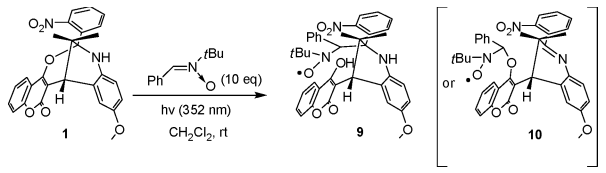

The atmospheric-pressure chemical ionization (APCI) mass spectroscopy (MS) measurements of the PBN spin-trapped species provided additional proof of the existence of the spin-trapped monoadduct. In the APCI-MS spectrum shown in Figure 10, only three apparent signals were detected. The signal

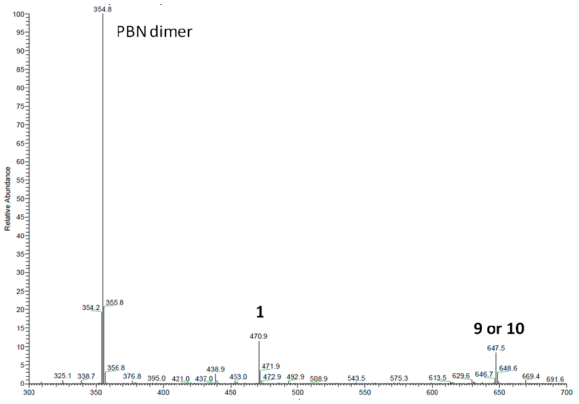

Figure 10. APCI-MS spectra of the PBN spin-trapped species **9** or **10**.

at *m*/*z* 648.6 was assigned to the adduct **9** or **10**, whereas the signals at *m*/*z* 354.8 and 470.9 were attributed to the PBN dimer and the oxazabicycle **1**, respectively. No signals for the bisadducts or any other spin-trapped species were observed in the mass spectra.

Characterization and Crystal Structures of the Side Products. For a better understanding of the photochemistry and its mechanism, we also investigated the photofatigue of the oxazabicycle **1** to retrieve mechanistic information from structural analyses of the photogenerated products. After prolonged irradiation of **1** in methylene chloride under UV irradiation (352 nm) for 1 day,[22] we were able to isolate and characterize the two photogenerated side products **11** and **12** (Figure 11). The X-ray crystal structure of **11** reveals the relocation of the C−O bond from the bridgehead to the *ipso* position of the anisidine ring along with a cyclohexadienone fragment, whereas **12** displays the presence of an indazole and a benzofuranone moiety on each side of the ring-opened form.

It is worth mentioning that the ^{13}C NMR spectra of **11** displayed two discernible absorptions at chemical shifts of 184.0 and 183.5 ppm. One was arbitrarily assigned to the carbonyl carbon of the cyclohexadienone moiety; the other, however, could not be reasonably accounted for. The ORTEP geometry-

dx.doi.org/10.1021/jo401838n | J. Org. Chem. 2013, 78, 11798−11806

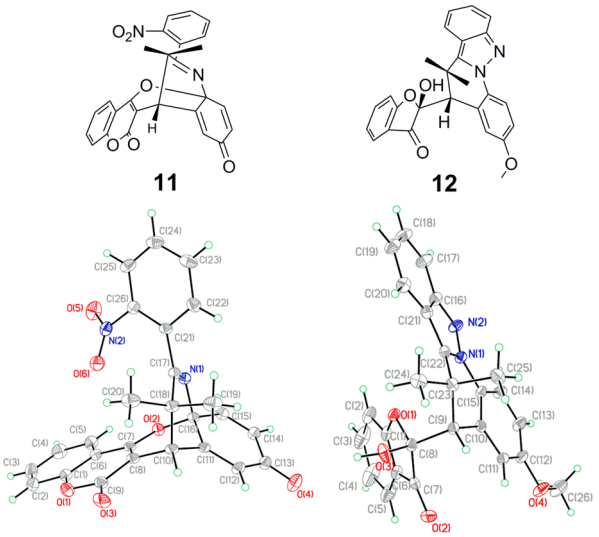

Figure 11. X-ray crystal structures of the two photogenerated side products **11** and **12**.

based quantum chemical calculations[23] of **11** suggested that this unjustifiable absorption could be attributed to the imine carbon adjacent to the nitrophenyl group. We assume that this unexpected 20 ppm downfield shift from the typical imine carbon absorption (160−165 ppm) probably resulted from its highly rigid bicyclic structure. In the literature, a similar observation has also been reported for rhazinoline, a highly strained indole alkaloid, whose imine carbon resonates even more downfield at 187.3 ppm in the ^{13}C NMR spectrum.[24] As for the photogenerated side product **12**, the X-ray crystallographic and NMR spectroscopic analyses indicated that it exists mainly in the lactol form in the solid state (Figure 11) but in the diketo form in solution (Scheme 6). Further, the diketo

Scheme 6. Equilibrium between the Lactol (12) and Diketo (12a) Species

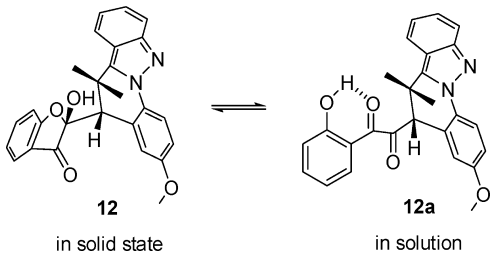

form **12a** was found to be the major isomer in $CDCl_3$, with a diketo to lactol ratio of approximately 10:1. This observation is in contrast to previous studies,[25] which suggested that the lactol form of 1-(2-hydroxyphenyl)propane-1,2-dione is the major isomer in aprotic solvents.

Scheme 7 outlines the proposed mechanism for the formation of the minor products **11** and **12** from exhaustive irradiation of **1**. Presumably, the oxygen radical **6** generated from **1** (Scheme 4) is trapped by the *ipso* carbon of the anisidine ring to form the cyclohexadiene radical **13**. The subsequent loss of one molecule of methane from **13** affords the zwitterionic biradical **14**.[26] Final charge neutralization via back electron transfer from the nitro radical anion to the iminium radical cation furnishes the product **11**. Alternately, the zwitterionic species **5** can also undergo light-mediated

Scheme 7. Proposed Mechanism for the Formation of 11 and 12

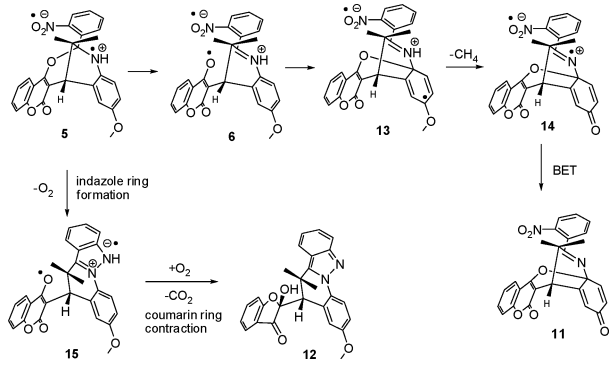

indazole ring formation. This reaction is realized by deoxygenation of the nitro group and followed by intramolecular N−N bond formation of the indazole ring to give the intermediate **15**.[27] The molecular oxygen released during indazole ring formation is then trapped in situ by the coumarin radical, which further undergoes ring contraction[25b] via decarboxylation to afford the product **12** (see Scheme S1 in the Supporting Information for mechanistic details).

Essentially, all functional groups present in the oxazabicycle **1** were found to participate in this photoreaction, though to varying extents: that is, the *o*-nitro group and the amine formed the indazole ring, the anisidine moiety was oxidized to the cyclohexadienone, and the coumarin underwent ring contraction to the benzofuranone. These observations also favor the proposed radical mechanism, since only radical species can be so indiscriminately reactive toward every functional group present in the molecular scaffold. On the basis of the aforementioned studies, it is suggested that the photochromism of **1** likely involves the zwitterionic biradical species **5** as the key transient intermediate, generated by photoinduced intramolecular electron transfer from the amine nitrogen to the *o*-nitrophenyl group. This unprecedented photochromic mechanism may potentially be utilized in the future design of organic photochromic colorants with novel molecular structures.

■ CONCLUSION

A one-pot preparation of the photochromic oxazabicycle **1** is presented. The successful trapping of the photogenerated product with trimethylsilyl cyanide confirms the formation of the zwitterionic species **2**. The results of EPR spectroscopic studies and spin-trapping experiments strongly support that the photochromism of **1** involves intramolecular electron transfer between the amine moiety and *o*-nitrophenyl group. Finally, two photodegradation side products, indazole **11** and cyclohexadienone **12**, were isolated and characterized, and a plausible mechanism for their formation from the zwitterionic biradical intermediate was also proposed. Further application of this photochromic mechanism in the design and synthesis of potential organic photochromic colorants is currently underway.

■ EXPERIMENTAL SECTION

General Experimental Considerations. Melting points were determined on a Mel-Temp melting point apparatus in open capillaries and are uncorrected. HRMS-EI measurement were performed on a spectrometer with a double-focusing magnetic sector mass analyzer. ESI and APCI-MS spectra were measured in the positive ion mode by

dx.doi.org/10.1021/jo401838n | J. Org. Chem. 2013, 78, 11798−11806

an LC-MS instrument with orbitrap mass analyzer. IR spectra were obtained using a FT-IR spectrophotometer. UV−vis spectra were measured on a spectrometer with photodiode array detector. Measurements of liquid-phase EPR spectra were performed on a CW-EPR spectrometer. Single-crystal structures were determined with an X-ray single-crystal diffractometer. ^{1}H and ^{13}C NMR spectra were recorded at 300 and 75 MHz on an FT-NMR spectrometer, respectively. Chemical shifts are reported in parts per million on the scale relative to an internal standard (tetramethylsilane, or appropriate solvent peaks), with coupling constants given in hertz. ^{1}H NMR multiplicity data are denoted by s (singlet), d (doublet), t (triplet), q (quartet), ABqd (AB quartet of doublets), and m (multiplet). Analytical thin-layer chromatography (TLC) was carried out on silica gel 60G-254 plates (25 mm) and developed with the solvents mentioned. Flash chromatography was performed in columns of various diameters with silica gel (230−400 mesh) by elution with the solvent systems. Solvents, unless otherwise specified, were reagent grade and were distilled once prior to use. All new compounds exhibited satisfactory spectroscopic and analytical data.

One-Pot Synthetic Procedure. To a solution of *p*-anisidine (500 mg, 4.06 mmol) in 1,2-dichloroethane (10 mL) was added 2-nitrobenzaldehyde (613 mg, 4.06 mmol), isobutyraldehyde (293 mg, 4.06 mmol), and a catalytic amount of *p*-TsOH (77 mg, 0.406 mmol) at room temperature. The mixture was stirred at that temperature for 12 h. 4-Hydroxycoumarin (658 mg, 4.06 mmol) was then added to the mixture, and the resulting solution was refluxed for 2 h. After it was cooled to room temperature, the reaction mixture was quenched with water (10 mL). The product was then extracted twice with methylene chloride (25 mL each). The combined organic extracts were dried over $MgSO_4$, filtered, and concentrated. The crude product was recrystallized in methylene chloride/ethyl acetate (1/6) or purified by column chromatography (1/9 EtOAc/hexanes) to give a yellow solid in 39% yield. The structural characterizations of **1** and **3** have been previously reported.[8]

Detection of the TMSCN Adduct. Compound **1** (5.0 mg, 10.6 μmol, dissolved in 0.7 mL of $CDCl_3$ in a quartz NMR tube) was irradiated with UV light (352 nm) at room temperature for 5 min. TMSCN (5.3 mg, 53.0 μmol) was then added to the solution. The resulting mixture was subjected to ^{1}H NMR spectroscopic measurements in an interval of 5−10 min under continuous irradiation. Another sample with the same treatment directly irradiated for 25 min was subjected to ^{1}H and ^{13}C NMR spectroscopic measurement.

TMSCN adduct **4**: ^{1}H NMR ($CDCl_3$, 300 MHz) δ 8.15 (dd, J = 8.7, 1.2 Hz, 1H), 7.68−7.64 (m, 2H), 7.56−7.51 (m, 3H), 7.35−7.21 (m, 3H), 6.79 (dd, J = 8.7, 2.7 Hz, 1H), 6.53 (dd, J = 8.7, 1.2 Hz, 1H), 5.00 (s, 1H), 3.86 (s, 1H), 3.75 (s, 3H), 1.17 (s, 3H), 0.99 (s, 3H); ^{13}C NMR ($CDCl_3$, 75 MHz) δ 171.2, 163.8, 161.5, 158.6, 153.0, 147.6, 136.9, 135.5, 133.6, 132.1, 130.4, 129.0, 128.5, 127.0, 124.7, 123.6, 117.7, 116.5, 113.5, 111.1, 110.4, 108.5, 55.3, 43.0, 41.0, 24.2, 22.1; APCI−HRMS m/z calcd for $C_{31}H_{32}N_3O_6Si$ [M + H$^+$] 570.2055, found 570.2052.

EPR Spectroscopy. The EPR spectra of **1**, **3**, **7**, and **8** were measured prior to and after irradiation with a mercury lamp at 365 nm through a quartz window in methylene chloride at 293 and 77 K. The EPR spectra were fitted using EasySpin (version 4.0.0), a computational package developed by Stoll and Schweiger. The EPR fitting procedure used a simplex type iteration to minimize the root-mean-square deviation.

Density Functional Theory (DFT) Calculations. Hybrid DFT calculations were carried out with the Gaussian 09 program[28] at the B3LYP level. The split-valence 6-31G(d,p) basis set was used for all elements unless specified. The geometry was determined by the ORTEP drawings of compounds **1** and **7**. Molecular orbital and spin density distribution was calculated with SCF density and visualized using GaussView (version 5.0.8).

Spin Trapping of the Biradical Intermediate. Compound **1** (1.0 mg, 2.1 μmol) dissolved in methylene chloride in a quartz tube (Φ 10 mm) was irradiated (352 nm) for 5 min at room temperature. PBN (3.7 mg, 21 μmol) was then added, and the resulting solution was subjected to APCI-MS determination and EPR measurements.

Electrochemistry and Spectroelectrochemical Studies. Electrochemistry was performed with a three-electrode potentiostat in THF with 0.1 M $TBAPF_6$ deoxygenated by purging with nitrogen gas. Cyclic voltammetry was conducted with the use of a homemade three-electrode cell equipped with a BAS glassy-carbon (0.07 cm^2) or platinum (0.02 cm^2) disk as the working electrode, a platinum wire as the auxiliary electrode, and a homemade Ag/AgCl (saturated) reference electrode. The reference electrode is separated from the bulk solution by a double junction filled with electrolyte solution. Potentials are reported vs Ag/AgCl (saturated) and referenced to the ferrocene/ferrocenium (Fc/Fc^+) couple, which occurs at $E_{1/2}$ = +0.57 V vs Ag/AgCl (saturated). The working electrode was polished with 0.03 μm aluminum on felt pads (Buehler) and was ultrasonicated for 1 min prior to each experiment. The reproducibility of individual potential values was within ±5 mV. The spectroelectrochemical experiments were accomplished with the use of a 1 mm cuvette, a 100 mesh platinum gauze as the working electrode, a platinum wire as the auxiliary electrode, and a Ag/AgCl (saturated) reference electrode.

Characterization of the Photogenerated Side Products. A solution of **1** (200 mg, 0.43 mmol) in 100 mL of MeCN was irradiated in a photoreactor (352 nm, 8 W x 8) at room temperature for 24 h. The solution was concentrated in vacuo, and the products were purified by column chromatography (gradient, 4/1 to 2/1 hexanes/EtOAc) to afford 14 mg (0.031 mmol, 7.1%) of compound **11** and 6 mg (0.014 mmol, 3.3%) of compound **12**.

*Compound **11**:* yellow solid; mp 170−172 °C; ^{1}H NMR ($CDCl_3$, 300 MHz) δ 8.15 (dd, J = 8.1, 1.5 Hz, 1H), 7.85 (dd, J = 8.1, 1.5 Hz, 1H), 7.69 (td, J = 7.5, 1.2 Hz, 1H), 7.62−7.55 (m, 2H), 7.42−7.36 (m, 2H), 7.31 (td, J = 7.8, 0.6 Hz, 1H), 6.48−6.44 (m, 2H), 3.89 (s, 1H), 1.43 (s, 3H), 1.23 (s, 3H); ^{13}C NMR ($CDCl_3$, 75 MHz) δ 184.0, 183.5, 162.3, 158.2, 152.8, 148.2, 146.8, 143.8, 133.6, 133.1, 132.7, 130.8, 129.9, 129.2, 125.2, 124.3, 124.0, 123.0, 116.7, 114.4, 101.1, 78.9, 53.4, 45.2, 27.4, 23.9; IR ν (KBr) 2963, 1712, 1603, 1505, 1251, 1043 cm^{-1}; HRMS (EI) m/z calcd for $C_{26}H_{18}N_2O_6$ [M$^+$] 454.1165, found 454.1160.

*Compound **12**:* white solid; mp 164−166 °C; ^{1}H NMR ($CDCl_3$, 300 MHz) δ 11.19 (s, 1H), 8.17 (d, J = 8.7 Hz, 1H), 7.79 (d, J = 8.7 Hz, 1H), 7.73 (d, J = 8.7 Hz, 1H), 7.44 (td, J = 8.7, 1.8 Hz, 1H), 7.29 (ddd, J = 9.0, 6.6, 1.2 Hz, 1H), 7.07−7.02 (m, 2H), 6.96−6.91 (m, 2H), 6.77 (d, J = 2.7 Hz, 1H), 6.65 (td, J = 8.1, 1.2 Hz, 1H), 4.57 (s, 1H), 3.72 (s, 3H), 2.01 (s, 3H), 1.39 (s, 3H); ^{13}C NMR ($CDCl_3$, 75 MHz) δ 196.0, 194.5, 163.6, 158.5, 149.4, 138.2, 135.9, 132.2, 129.8, 126.7, 123.3, 121.5, 120.7, 120.3, 119.6, 119.4, 118.2, 117.8, 115.6, 115.3, 115.0, 56.6, 55.6, 36.1, 28.8, 24.2; IR ν (KBr) 2965, 1721, 1611, 1505, 1258, 750 cm^{-1}; HRMS (EI) m/z calcd for $C_{26}H_{22}N_2O_4$ [M$^+$] 426.1580, found 426.1588.

Computational Details. Quantum chemical calculations were performed with the Gaussian 09 program package.[28] The ORTEP geometries of **11** were subjected to the theoretical calculations of ^{13}C NMR chemical shifts by using density functional theory (DFT) and the gauge-independent atomic orbital (GIAO) method at the MPW1PW91/6-31G basis set level and chloroform as the solvent with the IEF-PCM solvent continuum model. The results of the calculation were then compared with the experimental data.

■ ASSOCIATED CONTENT

Supporting Information

Figures, tables, and CIF files giving the X-ray crystal structure of **7**, HOMO/LUMO and spin density distributions of **1** and **7**, a proposed mechanism for the formation of **12** from **15**, calculated ^{13}C NMR data for **11**, additional spectra, and crystallographic data for **1**, **3**, **7**, **11**, and **12**. This material is available free of charge via the Internet at http://pubs.acs.org.

■ AUTHOR INFORMATION

Corresponding Author

*D.-Y.Y.: tel, 886-4-2359-7613; fax, 886-4-2359-0426; e-mail, yang@thu.edu.tw.

Notes

The authors declare no competing financial interest.

■ ACKNOWLEDGMENTS

We thank the National Science Council of the Republic of China, Taiwan, for financially supporting this research under Contract No. NSC 98-2113-M-029-003-MY2 as well as the National Center for High-performance Computing for computer time and facilities. We also thank Prof. Ping-Yu Chen for helpful discussions and assistance in the EPR simulations.

■ REFERENCES

(1) (a) Carroll, R.; Gorman, C. *Angew. Chem., Int. Ed.* **2002**, *41*, 4378. (b) Balzani, V.; Venturi, M.; Credi, A. *Molecular devices and machines: a journey into the nano world*; Wiley-VCH: Weinheim, Germany, 2003. (c) Margulies, D.; Felder, C.; Melman, G.; Shanzer, A. *J. Am. Chem. Soc.* **2007**, *129*, 347. (d) Feringa, B. L. *J. Org. Chem.* **2007**, *72*, 6635. (e) Szaciłowski, K. *Chem. Rev.* **2008**, *108*, 3481. (f) Areephong, J.; Hurenkamp, J.; Milder, M.; Meetsma, A.; Herek, J.; Browne, W.; Feringa, B. *Org. Lett.* **2009**, *11*, 721. (g) Baudrion, A.-L.; Perron, A.; Veltri, A.; Bouhelier, A.; Adam, P.-M.; Bachelot, R. *Nano Lett.* **2012**, *13*, 282. (h) Diaz, S. A.; Giordano, L.; Jovin, T. M.; Jares-Erijman, E. A. *Nano Lett.* **2012**, *12*, 3537.

(2) (a) Yokoyama, Y. *Chem. Rev.* **2000**, *100*, 1717. (b) Feringa, B. L.; Browne, W. R. *Molecular switches*, 2nd ed.; Wiley-VCH: Weinheim, Germany, 2011. (c) Raymo, F.; Tomasulo, M. *Chem. Eur. J.* **2006**, *12*, 3186. (d) Richmond, C. J.; Parenty, A. D. C.; Song, Y. F.; Cooke, G.; Cronin, L. *J. Am. Chem. Soc.* **2008**, *130*, 13059. (e) Gust, D.; Andreasson, J.; Pischel, U.; Moore, T. A.; Moore, A. L. *Chem. Commun.* **2012**, *48*, 1947.

(3) (a) Irie, M. *Chem. Rev.* **2000**, *100*, 1685. (b) Tanifuji, N.; Matsuda, K.; Irie, M. *Org. Lett.* **2005**, *7*, 3777. (c) Moriyama, Y.; Matsuda, K.; Tanifuji, N.; Irie, S.; Irie, M. *Org. Lett.* **2005**, *7*, 3315. (d) Sakamoto, R.; Kume, S.; Nishihara, H. *Chem. Eur. J.* **2008**, *14*, 6978. (e) Morinaka, K.; Ubukata, T.; Yokoyama, Y. *Org. Lett.* **2009**, *11*, 3890. (f) Tan, W.; Zhang, Q.; Zhang, J.; Tian, H. *Org. Lett.* **2009**, *11*, 161. (g) Nakashima, T.; Miyamura, K.; Sakai, T.; Kawai, T. *Chem. Eur. J.* **2009**, *15*, 1977. (h) Wong, H.; Ko, C.; Lam, W.; Zhu, N.; Yam, V. *Chem. Eur. J.* **2009**, *15*, 10005. (i) Delbaere, S.; Berthet, J.; Shiozawa, T.; Yokoyama, Y. *J. Org. Chem.* **2012**, *77*, 1853. (j) Suzuki, K.; Ubukata, T.; Yokoyama, Y. *Chem. Commun.* **2012**, *48*, 765. (k) Nakashima, T.; Kajiki, Y.; Fukumoto, S.; Taguchi, M.; Nagao, S.; Hirota, S.; Kawai, T. *J. Am. Chem. Soc.* **2012**, *134*, 19877. (l) Yang, Y.; Xie, Y.; Zhang, Q.; Nakatani, K.; Tian, H.; Zhu, W. *Chem. Eur. J.* **2012**, *18*, 11685. (m) Delbaere, S.; Berthet, J.; Shiozawa, T.; Yokoyama, Y. *J. Org. Chem.* **2012**, *77*, 1853. (n) Liu, G.; Pu, S.; Wang, R. *Org. Lett.* **2013**, *15*, 980.

(4) (a) Tanaka, M.; Nakamura, M.; Salhin, M.; Ikeda, T.; Kamada, K.; Ando, H.; Shibutani, Y.; Kimura, K. *J. Org. Chem.* **2001**, *66*, 1533. (b) Minkin, V. *Chem. Rev.* **2004**, *104*, 2751. (c) Tomasulo, M.; Sortino, S.; White, A.; Raymo, F. *J. Org. Chem.* **2005**, *70*, 8180. (d) Nagashima, S.; Murata, M.; Nishihara, H. *Angew. Chem., Int. Ed.* **2006**, *45*, 4298. (e) Darwish, T. A.; Evans, R. A.; James, M.; Malic, N.; Triani, G.; Hanley, T. L. *J. Am. Chem. Soc.* **2010**, *132*, 10748. (f) Patel, D. G.; Paquette, M. M.; Kopelman, R. A.; Kaminsky, W.; Ferguson, M. J.; Frank, N. L. *J. Am. Chem. Soc.* **2010**, *132*, 12568.

(5) (a) Kurihara, M.; Hirooka, A.; Kume, S.; Sugimoto, M.; Nishihara, H. *J. Am. Chem. Soc.* **2002**, *124*, 8800. (b) Siewertsen, R.; Neumann, H.; Buchheim-Stehn, B.; Herges, R.; Näther, C.; Renth, F.; Temps, F. *J. Am. Chem. Soc.* **2009**, *131*, 15594. (c) Beharry, A. A.; Wong, L.; Tropepe, V.; Woolley, G. A. *Angew. Chem., Int. Ed.* **2011**, *50*, 1325. (d) Hashim, P. K.; Tamaoki, N. *Angew. Chem., Int. Ed.* **2011**, *50*, 11729. (e) Takaishi, K.; Kawamoto, M.; Muranaka, A.; Uchiyama, M. *Org. Lett.* **2012**, *14*, 3252. (f) Kamei, T.; Fukaminato, T.; Tamaoki, N. *Chem. Commun.* **2012**, *48*, 7625. (g) Samanta, S.; Beharry, A. A.; Sadovski, O.; McCormick, T. M.; Babalhavaeji, A.; Tropepe, V.; Woolley, G. A. *J. Am. Chem. Soc.* **2013**, *135*, 9777.

(6) (a) Feringa, B.; van Delden, R.; Koumura, N.; Geertsema, E. *Chem. Rev.* **2000**, *100*, 1789. (b) Wang, Z.; Todd, E.; Meng, X.; Gao, J. *J. Am. Chem. Soc.* **2005**, *127*, 11552. (c) Biedermann, P.; Stezowski, J.; Agranat, I. *Chem. Eur. J.* **2006**, *12*, 3345. (d) Fukui, M.; Mori, T.; Inoue, Y.; Rathore, R. *Org. Lett.* **2007**, *9*, 3977. (e) Jiang, X.; Lim, Y.; Zhang, B.; Opsitnick, E.; Baik, M.; Lee, D. *J. Am. Chem. Soc.* **2008**, *130*, 16812. (f) Canary, J. *Chem. Soc. Rev.* **2009**, *38*, 747. (g) Tietze, L.; Düfert, A.; Lotz, F.; Sölter, L.; Oum, K.; Lenzer, T.; Beck, T.; Herbst-Irmer, R. *J. Am. Chem. Soc.* **2009**, *131*, 17879.

(7) (a) Kikuchi, A.; Iwahori, F.; Abe, J. *J. Am. Chem. Soc.* **2004**, *126*, 6526. (b) Fölling, J.; Belov, V.; Kunetsky, R.; Medda, R.; Schönle, A.; Egner, A.; Eggeling, C.; Bossi, M.; Hell, S. *Angew. Chem., Int. Ed.* **2007**, *46*, 6266. (c) Sousa, C. M.; Pina, J.; de Melo, J. S.; Berthet, J.; Delbaere, S.; Coelho, P. J. *Org. Lett.* **2011**, *13*, 4040. (d) Fukaminato, T.; Tateyama, E.; Tamaoki, N. *Chem. Commun.* **2012**, *48*, 10874. (e) Shrestha, T. B.; Kalita, M.; Pokhrel, M. R.; Liu, Y.; Troyer, D. L.; Turro, C.; Bossmann, S. H.; Dürr, H. *J. Org. Chem.* **2012**, *78*, 1903. (f) Hatano, S.; Horino, T.; Tokita, A.; Oshima, T.; Abe, J. *J. Am. Chem. Soc.* **2013**, *135*, 3164. (g) Sousa, C. M.; Berthet, J.; Delbaere, S.; Coelho, P. J. *J. Org. Chem.* **2013**, *78*, 6956.

(8) Yang, D. Y.; Chen, Y. S.; Kuo, P. Y.; Lai, J. T.; Jiang, C. M.; Lai, C. H.; Liao, Y. H.; Chou, P. T. *Org. Lett.* **2007**, *9*, 5287.

(9) Lai, J. T.; Shieh, P. S.; Huang, W. H.; Yang, D. Y. *J. Comb. Chem.* **2008**, *10*, 381.

(10) Crystallographic data (excluding structure factors) for **1**, **3**, **7**, **11**, and **12** have been deposited with the Cambridge Crystallographic Data Centre as supplementary publication numbers CCDC 928960, 928961, 686994, 928962, and 928963, respectively. These data can be obtained free of charge via www.ccdc.cam.ac.uk/data_request/cif, by e-mailing data_request@ccdc.cam.ac.uk, or by contacting The Cambridge Crystallographic Data Centre, 12 Union Road, Cambridge CB2 1EZ, U.K. (fax: +44 1223 336033).

(11) Malatesta, V.; Neri, C.; Wis, M. L.; Montanari, L.; Millini, R. *J. Am. Chem. Soc.* **1997**, *119*, 3451.

(12) Stoll, S.; Schweiger, A. *J. Magn. Reson.* **2006**, *178*, 42.

(13) Kumar, S.; Engman, L.; Valgimigli, L.; Amorati, R.; Fumo, M. G.; Pedulli, G. F. *J. Org. Chem.* **2007**, *72*, 6046.

(14) Neta, P.; Fessenden, R. W. *J. Phys. Chem.* **1974**, *78*, 523.

(15) Nelsen, S. F.; Landis, R. T.; Kiehle, L. H.; Leung, T. H. *J. Am. Chem. Soc.* **1972**, *94*, 1610.

(16) Chen, W. Z.; Wei, H. Y.; Yang, D. Y. *Tetrahedron* **2013**, *69*, 2775.

(17) (a) Yoon, U. C.; Kwon, H. C.; Hyung, T. G.; Choi, K. H.; Oh, S. W.; Yang, S.; Zhao, Z.; Mariano, P. S. *J. Am. Chem. Soc.* **2004**, *126*, 1110. (b) Yong, P. K.; Banerjee, A. *Org. Lett.* **2005**, *7*, 2485.

(18) (a) Jonsson, M.; Lind, J.; Eriksen, T. E.; Merenyi, G. *J. Am. Chem. Soc.* **1994**, *116*, 1423. (b) Goto, M.; Otsuka, K.; Chen, X.; Tao, Y.; Oyama, M. *J. Phys. Chem. A* **2004**, *108*, 3980.

(19) (a) Kaim, W.; Fiedler, J. *Chem. Soc. Rev.* **2009**, *38*, 3373. (b) Lee, C. W.; Lu, H. P.; Lan, C. M.; Huang, Y. L.; Liang, Y. R.; Yen, W. N.; Liu, Y. C.; Lin, Y. S.; Diau, E. W.; Yeh, C. Y. *Chem. Eur. J.* **2009**, *15*, 1403. (c) Mutoh, K.; Nakano, E.; Abe, J. *J. Phys. Chem. A* **2012**, *116*, 6792.

(20) (a) Makarova, K.; Rokhina, E. V.; Golovina, E. A.; Van As, H.; Virkutyte, J. *J. Phys. Chem. A* **2012**, *116*, 443. (b) Flores, M.; Okamura, M. Y.; Niklas, J.; Pandelia, M. E.; Lubitz, W. *J. Phys. Chem. B* **2012**, *116*, 8890. (c) Fraind, A. M.; Sini, G.; Risko, C.; Ryzhkov, L. R.; Bredas, J. L.; Tovar, J. D. *J. Phys. Chem. B* **2013**, *117*, 6304. (d) Liu, G.; Gimenez-Lopez, M. d. C.; Jevric, M.; Khlobystov, A. N.; Briggs, G. A.; Porfyrakis, K. *J. Phys. Chem. B* **2013**, *117*, 5925.

(21) (a) Branchadell, V.; Font, J.; Moglioni, A. G.; Ochoa de Echagüen, C.; Oliva, A.; Ortuño, R. M.; Veciana, J.; Vidal-Gancedo, J. *J. Am. Chem. Soc.* **1997**, *119*, 9992. (b) Liu, Y. P.; Wang, L. F.; Nie, Z.; Ji, Y. Q.; Liu, Y.; Liu, K. J.; Tian, Q. *J. Org. Chem.* **2006**, *71*, 7753. (c) Usuki, T.; Nakanishi, K.; Ellestad, G. A. *Org. Lett.* **2006**, *8*, 5461. (d) Rosenau, T.; Kloser, E.; Gille, L.; Mazzini, F.; Netscher, T. *J. Org. Chem.* **2007**, *72*, 3268. (e) Malval, J.-P.; Morlet-Savary, F.; Chaumeil, H. l. n.; Balan, L.; Versace, D.-L.; Jin, M.; Defoin, A. *J. Phys. Chem. C* **2009**, *113*, 20812. (f) Polyakov, N. E.; Leshina, T. V.; Meteleva, E. S.;

Dushkin, A. V.; Konovalova, T. A.; Kispert, L. D. *J. Phys. Chem. B* **2010**, *114*, 14200.
(22) (a) Naumov, P.; Ohashi, Y. *J. Phys. Org. Chem.* **2004**, *17*, 865. (b) Sajimon, M. C.; Ramaiah, D.; Suresh, C. H.; Adam, W.; Lewis, F. D.; George, M. V. *J. Am. Chem. Soc.* **2007**, *129*, 9439.
(23) (a) Bagno, A.; Rastrelli, F.; Saielli, G. *Chem. Eur. J.* **2006**, *12*, 5514. (b) Festa, C.; De Marino, S.; Sepe, V.; D'Auria, M. V.; Bifulco, G.; Débitus, C.; Bucci, M.; Vellecco, V.; Zampella, A. *Org. Lett.* **2011**, *13*, 1532. (c) Lodewyk, M. W.; Siebert, M. R.; Tantillo, D. J. *Chem. Rev.* **2011**, *112*, 1839. (d) Leroyer, L.; Lepetit, C.; Rives, A.; Maraval, V.; Saffon-Merceron, N.; Kandaskalov, D.; Kieffer, D.; Chauvin, R. *Chem. Eur. J.* **2012**, *18*, 3226. (e) Ji, N.-Y.; Liu, X.-H.; Miao, F.-P.; Qiao, M.-F. *Org. Lett.* **2013**, *15*, 2327.
(24) Lim, K. H.; Hiraku, O.; Komiyama, K.; Koyano, T.; Hayashi, M.; Kam, T. S. *J. Nat. Prod.* **2007**, *70*, 1302.
(25) (a) Brewer, J.; Davidson, W.; Elix, J.; Leppik, R. *Aust. J. Chem.* **1971**, *24*, 1883. (b) Frimer, A. A.; Marks, V.; Gilinsky-Sharon, P.; Aljadeff, L.; Gottlieb, H. E. *J. Org. Chem.* **1995**, *60*, 4510.
(26) Gámez-Montaño, R.; Ibarra-Rivera, T.; Kaïm, L. E.; Miranda, L. D. *Synthesis* **2010**, 1285.
(27) Lin, W.-C.; Yang, D.-Y. *Org. Lett.* **2013**, *15*, 4862.
(28) Frisch, M. J.; Trucks, G. W.; Schlegel, H. B.; Scuseria, G. E.; Robb, M. A.; Cheeseman, J. R.; Scalmani, G.; Barone, V.; Mennucci, B.; Petersson, G. A.; Nakatsuji, H.; Caricato, M.; Li, X.; Hratchian, H. P.; Izmaylov, A. F.; Bloino, J.; Zheng, G.; Sonnenberg, J. L.; Hada, M.; Ehara, M.; Toyota, K.; Fukuda, R.; Hasegawa, J.; Ishida, M.; Nakajima, T.; Honda, Y.; Kitao, O.; Nakai, H.; Vreven, T.; Montgomery, J. A., Jr.; Peralta, J. E.; Ogliaro, F.; Bearpark, M.; Heyd, J. J.; Brothers, E.; Kudin, K. N.; Staroverov, V. N.; Kobayashi, R.; Normand, J.; Raghavachari, K.; Rendell, A.; Burant, J. C.; Iyengar, S. S.; Tomasi, J.; Cossi, M.; Rega, N.; Millam, J. M.; Klene, M.; Knox, J. E.; Cross, J. B.; Bakken, V.; Adamo, C.; Jaramillo, J.; Gomperts, R.; Stratmann, R. E.; Yazyev, O.; Austin, A. J.; Cammi, R.; Pomelli, C.; Ochterski, J. W.; Martin, R. L.; Morokuma, K.; Zakrzewski, V. G.; Voth, G. A.; Salvador, P.; Dannenberg, J. J.; Dapprich, S.; Daniels, A. D.; Ö. Farkas, Foresman, J. B.; Ortiz, J. V.; Cioslowski, J.; , and Fox, D. J. *Gaussian 09, Revision A.1*, Gaussian, Inc., Wallingford, CT, 2009.